Journal of Catalysis **200,** 59–68 (2001)
doi:10.1006/jcat.2001.3199, available online at http://www.idealibrary.com on IDEAL®

Deposition of Highly Dispersed Gold on Alumina Support

Yeong-Jey Chen and Chuin-tih Yeh[1]

Department of Chemistry, National Tsinghua University, Hsinchu, Taiwan, Republic of China

Received July 31, 2000; revised December 5, 2000; accepted February 5, 2001; published online April 18, 2001

Gold catalysts of Au/Al_2O_3, prepared by the methods of deposition precipitation (DP, $AuCl_3$ was the precursor of gold) and chemical vapor deposition (CVD, an organic gold complex was the precursor), were tested in the reaction of CO oxidation at subambient temperatures. The activity observed for prepared catalysts generally increased with their gold dispersion characterized by transmission electron microscopy. Finely dispersed Au/Al_2O_3 (with $d_{Au} < 5$ nm) catalysts may be easily prepared by the CVD method. Au/Al_2O_3 samples prepared by the traditional DP method contained many large gold crystallites ($d_{Au} > 7$ nm). They originated, during the impregnation step, from the occlusion of gold complex solution in pores of Al_2O_3. However, small gold particles ($d_{Au} \sim 3.5$ nm) may be deposited on Al_2O_3 by a modified DP method featuring prealkalinization of the Al_2O_3 surface. Furthermore, a mild hydrogen reduction is effective in eliminating the incubation period required for catalysts freshly prepared by the DP method. Characterization of the temperature-programmed reduction revealed that the function of reduction was to remove poisonous chloride ions from deposited gold crystallites. © 2001 Academic Press

Key Words: **CO oxidation; gold catalyst; pretreatment; activation.**

1. INTRODUCTION

The element gold has long been regarded as an inert metal that is catalytically less active than most transition metals (1, 2). Recently, Haruta *et al.* found that nanoparticles of gold dispersed on porous oxides were active toward the oxidation of carbon monoxide at subambient temperatures (3–5):

$$2CO + O_2 \rightarrow 2CO_2. \qquad [1]$$

The catalytic performance of these catalysts depends markedly on the particle size of gold, the nature of the supports, and the interaction between gold particles and support surface. Consequently, catalytic properties of gold are influenced significantly by preparative parameters.

The catalytic activity of gold catalysts generally increases with decreasing size of dispersed gold particles. Several methods have been proposed for preparation of highly dispersed ($d < 5$ nm) gold catalysts (4, 6–12) that have good CO oxidation activity at subambient temperatures. Among the techniques proposed, deposition–precipitation (DP) is the conventional method of prparing highly dispersed gold on oxide supports such as TiO_2 and MgO. However, this traditional method usually deposits large ($d > 7$ nm) gold crystallites when dispersed on alumina, the support most commonly used in industrial catalysts (13).

It is therefore the goal of this study to prepare highly dispersed Au/Al_2O_3 catalysts. This goal has been successfully accomplished by a modified deposition–precipitation method and the technique of chemical vapor deposition.

Pretreatment is generally required for activation of gold catalysts prepared from the precursor of $AuCl_3$ (14, 15). Usually, prereduction yields higher CO conversion at room temperature than preoxidation (15). In this study, we found that temperature-programmed reduction is useful in determining the appropriate reduction conditions for removing chloride poison while preserving the dispersion of gold crystallites.

2. METHODS

2.1. Catalyst Preparation

Two kinds of metal oxide, γ-Al_2O_3 (Kaiser, S.A. = 234 m^2/g) and TiO_2, were used as supports in this study. TiO_2 powder was synthesized in the laboratory by hydrolysis of $Ti(i\text{-}OC_3H_7)_4$ (Acros Chem. Co., 98%).

The traditional method of DP of gold onto supports may be found in the literature (6). In our laboratory, 5 ml of 0.1 M $AuCl_3$ (Aldrich Chem. Co., 99%) aqueous solution was added to 5 g oxide support suspended in deionized water to prepare 2 wt% gold catalysts. The pH of the solution was then adjusted to 7 with 0.1 M NaOH for depositing Au ions onto the support surface (6). After 2 h of stirring at 343 K, impregnated samples were filtered, washed with deionized water (until no AgCl precipitate was noted on dropping the filtrate into an $AgNO_3$ solution), and then dried for 12 h at 373 K in air. These dried powders were stored as fresh samples for further physical characterization and catalytic activity measurements.

---

[1] To whom correspondence should be addressed. E-mail: ctyeh@mx.nthu.edu.tw. Fax: 886-3-5726047.

0021-9517/01 $35.00

In a modified deposition–precipitation (referred to hereafter as modified DP) method, alumina powders were suspended in deionized water and the pH of the suspension was preadjusted to 7 with 0.1 M NaOH. An aqueous solution of 0.1 M $AuCl_3$ was subsequently added drop by drop into the neutralized suspension, along with a 0.1 M NaOH solution to maintain a pH of 7. After 2 h stirring at 343 K, impregnated samples were filtered, washed, dried at 373 K, and stored as fresh samples.

Chemical vapor deposition (CVD) was performed in a vacuum system using an organic complex, dimethyl–gold(III)–acetyl acetonate [DMGAA, $(CH_3)_2Au(CH_3COCH_2COCH_3)$ from Strem Chem. Co.] as the gold precursor. Support powders (around 2 g) were preevacuated at 473 K for 4 h to remove adsorbed water and then calcined for 30 min in 20 Torr O_2 at 473 K to remove organic contamination. The organic gold precursor was gradually evaporated, at 343 K, from the precursor vessel and adsorbed onto the surface of the support through the vacuum system. The deposition generally lasted 24 h, and the resulting samples were stored after calcination at 573 K in air to burn out organic ligands in the gold precursor.

2.2. Physical Characterization

The thermal decomposition of organic ligands from CVD samples was examined by thermogravimetric and differential thermal analysis (TG/DTA) (Seiko SSC 5000) at a heating rate of 10 K/min in a flow of air. The crystalline structure of supports was examined by X-ray diffraction (XRD, Shimadzu XD-5 with 0.154-nm line of Cu*K*). The gold loading on each sample was analyzed, after digestion in aqua regia, with a Perkin–Elmer 5500 atomic absorption spectrometer. The particle size of supported gold was examined by transmission electron microscopy (TEM; JEOL JEM-4000EX).

Temperature-programmed reduction (TPR) was performed in a fixed-bed reactor. A fresh sample of 0.20 g was inserted into quartz tubing of 6-mm i.d. After a 30-min purge with nitrogen gas, the TPR trace was pursued in a 30 ml/min flow of 5% H_2 in nitrogen on raising the system temperature from 300 K at the rate of 7 K/min. The rate of hydrogen consumption during TPR characterization was monitored with a thermal conductivity detector (TCD).

2.3. Catalytic Activities

The catalytic activity of prepared samples toward CO oxidation was tested in a fixed-bed flow reactor. The reactant gas, a 33 ml/min flow of 1 vol% CO in air, was catalyzed by a powder sample (0.10 g) packed in a quartz tube (space velocity $= 2 \times 10^4$ ml/g cat $\cdot$ h) of 4-mm i.d. The reaction temperature was controlled by a thermal couple (1.2-mm i.d.) in contact with the inlet of the catalyst bed. A stabilization period of 1 h was allowed before the analysis of product composition. The fraction of carbon monoxide remaining in the product was analyzed by gas chromatography (China Chrom. Co., 8700T) using a TCD and a 5-m column of Molecular Sieve 13X.

3. RESULTS

3.1. Calcination of Titania Support

$Ti(i\text{-}OC_3H_7)_4$ precursor was hydrolyzed in deionized water to prepare $Ti(OH)_4$ precipitate. Two endothermically weight loss signals, at 333 and 473 K, respectively, were noted in the TG/DTA spectrum of the precipitate dried at 333 K (Fig. 1). These signals indicated the dehydration of $Ti(OH)_4$ to TiO_2.

Figure 2 shows that the initially dehydrated TiO_2 was XRD amorphous, but became crystallized after calcination at elevated temperatures (T_c) in air. Two diffraction peaks with diffraction angles between $2\theta = 20^\circ$ and 30° were found from calcined samples. The peak at $2\theta = 25.3^\circ$ belongs to the anatase $TiO_2(101)$, and the peak at $2\theta = 27.5^\circ$ comes from the rutile $TiO_2(110)$.

BET characterization revealed that the surface area of TiO_2 decreased from 140 m^2/g (M-TiO_2, $T_c = 473$ K) to 47 m^2/g (N-TiO_2, $T_c = 873$ K) on raising T_c. Transmission electron micrographs (Figs. 3a and 3b) show that calcined samples were agglomerated from primary TiO_2 particles of 2–10 nm (M-TiO_2) and 10–40 nm (N-TiO_2), respectively.

3.2. Characterization of Gold Catalysts

Table 1 lists gold samples prepared in this study along with their properties. The seven supported samples studied are listed in the first column of this table with two capital letters. The first letter indicates the kind of support (M, N, and A represent M-TiO_2, N-TiO_2, and γ-Al_2O_3, respectively) and the second letter indicates the method of sample preparation (D, M, and C represent DP, modified

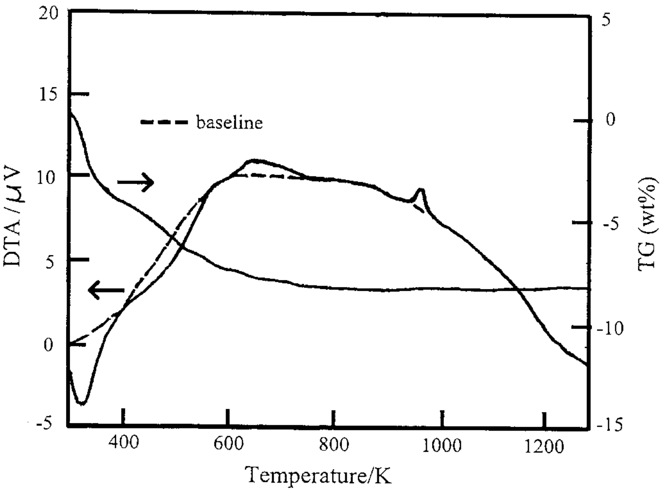

FIG. 1. TG/DTA results for 333 K dried $Ti(OH)_4$.

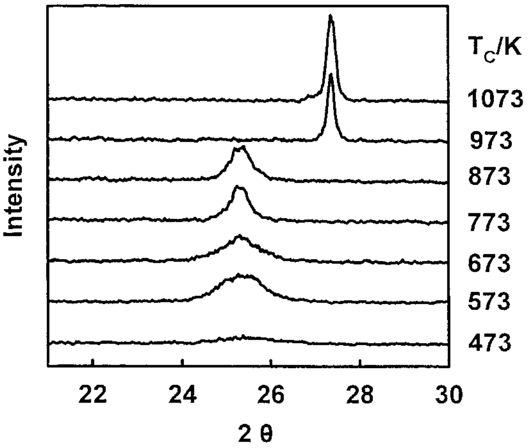

FIG. 2. XRD spectra obtained from titania calcined at different temperatures in air.

DP, and CVD, respectively). The fourth column of Table 1 lists the loading of gold analyzed by atomic absorption (AA) spectrometry. Only a portion of the gold from the precursor was found deposited on samples (to form intended 2.0 wt%) prepared by the DP method.

In Fig. 4 are histograms of the gold particles counted in transmission electron micrographs of prepared sample (Figs. 3c–3i). The fifth column of Table 1 lists the arithmetically averaged diameters obtained from the histograms. The gold clusters on samples prepared by CVD are generally smaller and the size distribution is more homogeneous than for those prepared by the DP method. Surprisingly, sample AM, the Au/Al_2O_3 prepared by the modified DP method, displayed higher Au dispersion than sample AC.

Figure 5 compares TPR traces obtained from four fresh samples prepared by the DP method. A hydrogen consumption signal was noted in each trace. Gold complexes deposited on Au/TiO_2 and Au/Al_2O_3 were reduced around 373 and 473 K, respectively. Obviously, the temperature required for reduction of gold precursors varied with the kind of support.

Figure 6 shows the TG/DTA results for NC sample freshly prepared by the CVD method. An exothermic weight loss process (due to combustion of DMGAA precursor) was noted at 573 K. No reductive signal was observed in a subsequent TPR experiments with all oxidized CVD samples.

3.3. *Catalytic Activity at 273 K*

The initial activity of freshly prepared catalysts toward CO oxidation at 273 K varied significantly with preparation parameters. All of the CVD samples (MC, NC, and AC) displayed 100% initial conversion of CO after burnout of organic ligands (calcination at 573 K). Catalysts prepared by the DP method (AD, AM, MD, and ND) were completely inactive at the beginning (Fig. 7). However, Au/TiO_2 samples (MD and ND) were activated by the reactant flow and reached 100% CO conversion after an incubation period of about 2 h. This pretreatment was definitely too mild for activation of Au/Al_2O_3 samples (AD and AM). No sign of activation was observed by treating them in the reactant flow.

Prereduction with a flow of hydrogen before the activity test was then attempted on catalysts prepared by the DP method. The temperatures of hydrogen consumption illustrated in Fig. 5 (373 and 473 K for Au/TiO_2 and Au/Al_2O_3, respectively) were accepted as the temperatures of prereduction treatment. Figure 8 is the time profile of CO conversion from prereduced samples. After the prereduction, samples MD, ND (Au/TiO_2), and AM (Au/Al_2O_3 prepared by modified DP) showed excellent initial activity. The incubation period required in Fig. 7 for Au/TiO_2 was successfully eliminated. Notably, although sample AM could be activated by the prereduction, sample AD (Au/Al_2O_3 prepared with the DP method) remained inactive at a reaction temperature of 273 K.

3.4. *Effect of Reaction Temperature*

CO oxidation was subsequently tested at elevated temperatures for the prereduced AD catalyst. Significant CO conversion was observed for this catalyst on raising the temperature over 300 K. Obviously, the catalytic activity of this catalyst was too low at 273 K but increased with the temperature of reaction. A small activation energy is required for the initiation of this exothermic reaction. Figure 9 compares the temperature profiles of CO conversion over reduced samples prepared by the DP method. Similar profiles were also obtained for the oxidized samples prepared by the CVD method (Fig. 10). Conversion of all of these catalysts increased with reaction temperature. However,

TABLE 1

Preparation Conditions and Characterization Results for the Gold Catalyst Samples Studied

Sample	Support	Preparation method	Au (wt%)	d^a (nm)	T_r^b (K)	$N_{H_2}/1.5N_{Au}^c$	$T_{1/2}^d$ (K)
MD	M-TiO_2	DP	1.01	4.3 ± 1.0	355	0.38	247
ND	N-TiO_2	DP	0.40	4.7 ± 1.1	328	0.36	249
AD	γ-Al_2O_3	DP	1.32	7.2 ± 2.6	465	0.46	296
AM	γ-Al_2O_3	Modified DP	1.73	3.4 ± 1.7	455	0.46	236
MC	M-TiO_2	CVD	4.37	2.8 ± 1.0	—[e]	—	209
NC	N-TiO_2	CVD	3.36	3.8 ± 1.1	—	—	230
AC	γ-Al_2O_3	CVD	4.58	4.1 ± 1.7	—	—	252

[a] Detected by TEM.

[b] Reduction temperature of samples detected by TPR.

[c] N_{H_2} and N_{Au} denote the number of hydrogen molecules consumed in TPR trace and the number of Au atoms in fresh samples, respectively.

[d] Temperature required for 50% CO conversion.

[e] —, No TPR signal was observed.

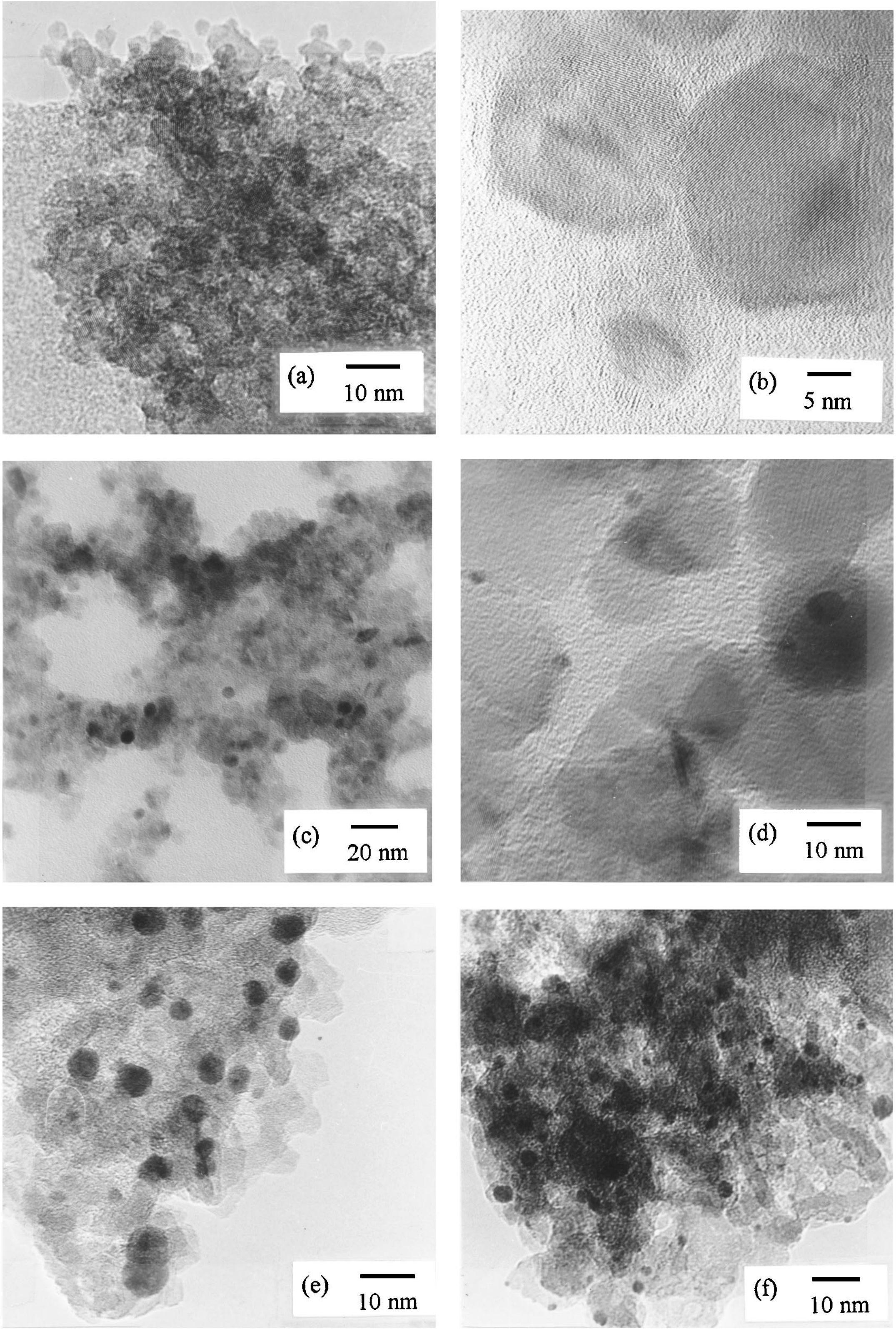

FIG. 3. Transmission electron micrographs of (a) amorphous TiO_2, (b) anatase TiO_2 supports, and (c) MD, (d) ND, (e) AD, (f) AM, (g) MC, (h) NC, (i) AC fresh samples. (j) The existence of fringe pattern from a good crystallite on sample ND dried at 373 K.

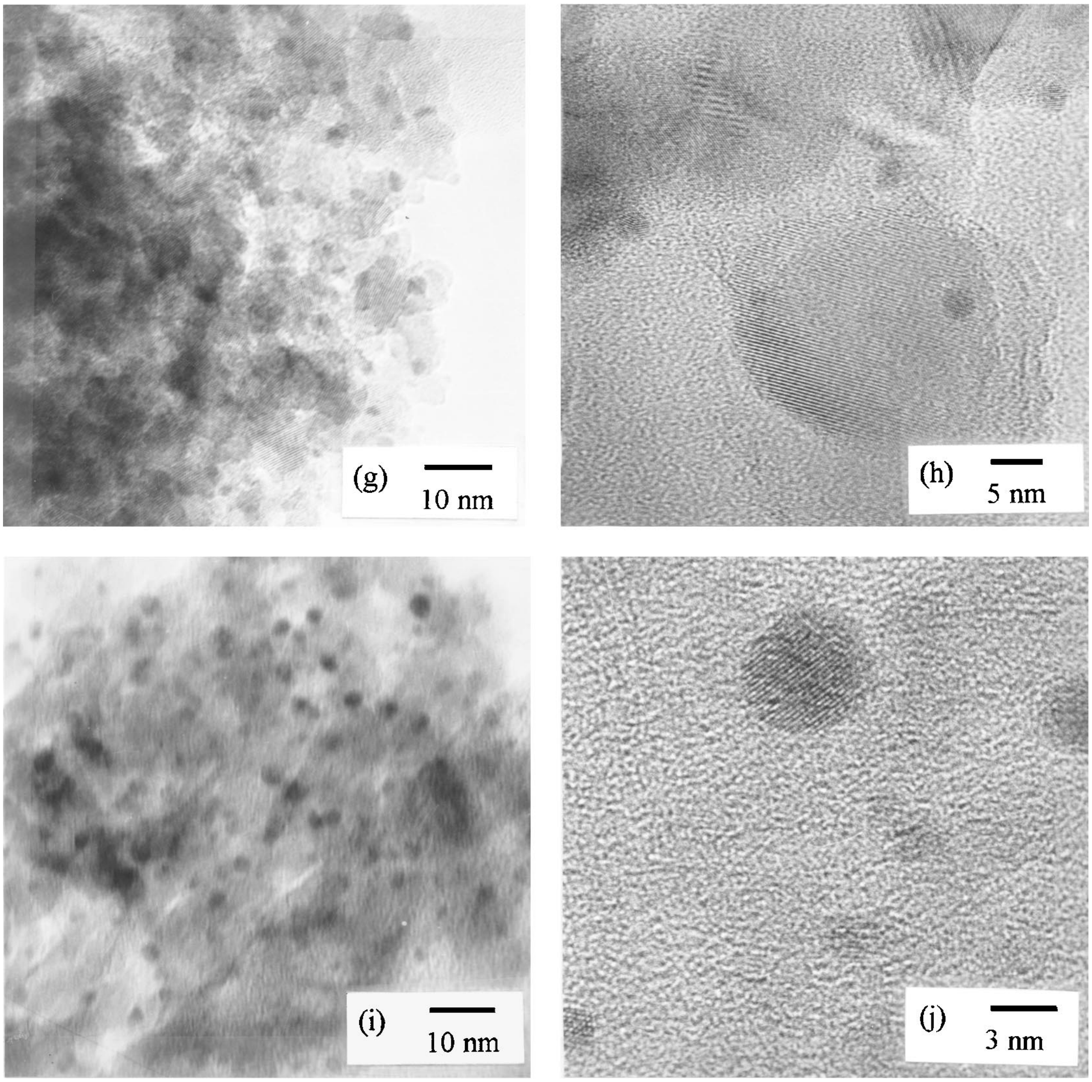

FIG. 3.—*Continued*

the temperature required for the same conversion varied with the nature of the prepared samples. The last column of Table 1 compares the temperatures required by each catalyst for 50% CO conversion ($T_{1/2}$). Sample MC (Au/M-TiO_2 prepared by the CVD) exhibited the lowest $T_{1/2}$ and could catalyze CO oxidation even at 200 K.

4. DISCUSSION

4.1. The Phase Transfer of TiO_2 on Calcination

Two endothermic transitions (333 K and 473 K) were observed in the TG/TDA spectra of $Ti(OH)_4$ (Fig. 1). From the total weight loss during these transitions (~8%), they come from dehydration of $Ti(OH)_4$ to TiO_2, i.e.,

$$\mathrm{Ti(OH)_4} \xrightarrow{473\mathrm{K}} \mathrm{TiO_2} + 2\mathrm{H_2O}. \qquad [2]$$

Figure 2 indicates that $Ti(OH)_4$ was dehydrated into amorphous TiO_2 after calcination at $T_c = 473$ K. The amorphous TiO_2 gradually converted to the anatase phase at higher temperatures and finally transformed into the rutile phase at $T_c \geq 973$ K.

The width of diffraction peaks in Fig. 2 narrowed with T_c of the calcination treatment. Obviously, TiO_2 crystallites gradually sintered into large particles on raising T_c. The sintering is confirmed by a decrease in BET surface area and an increase in the particle size of primary particles found in TEM (Figs. 3a and 3b).

4.2. The Process of Deposition Precipitation

A dissolution of $AuCl_3$ precursor in water may yield six kinds of possible gold species, i.e., five dissolved $AuCl_x(OH)_{4-x}^-$ complexes (with $x < 4$) in the solution and a $AuCl_y(OH)_{3-y}$ precipitate (with $y < 1.0$). The relative

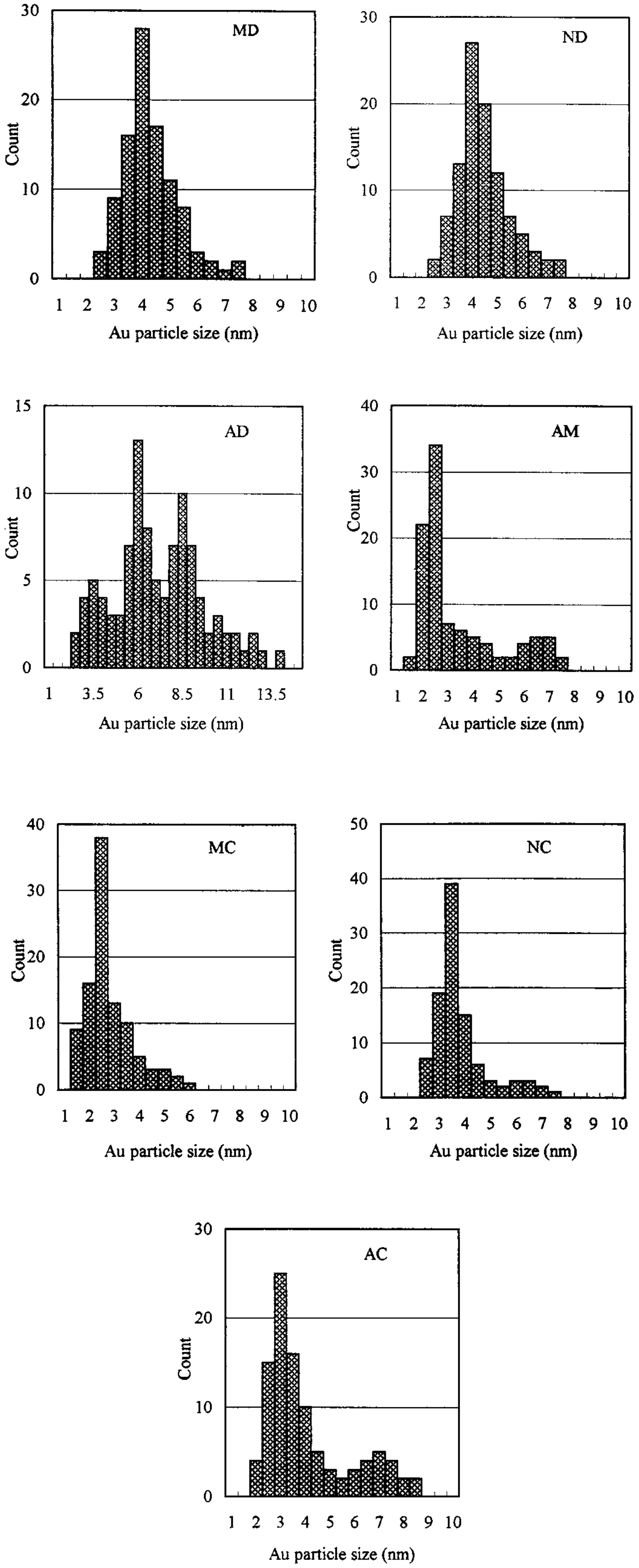

FIG. 4. Histograms of gold particle size observed in transmission electron micrographs of fresh samples.

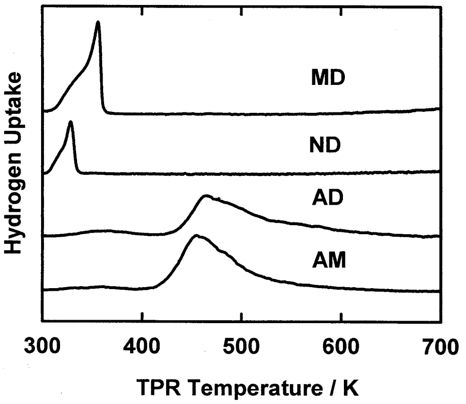

FIG. 5. TPR traces observed for fresh samples prepared by DP method.

contributions of these species varied with the pH value of the $AuCl_3$ solution (13). At pH 7.0 (optimized pH value for a decent gold deposition), the $AuCl_y(OH)_{3-y}$ precipitate as well as the complexes of $AuCl(OH)_3^-$ and $Au(OH)_4^-$ are major gold species in the solution system under thermodynamic equilibrium. Accordingly, on adjusting the support (alumina or titania) suspended solution of $AuCl_3$ to this pH value, the pores of the support should be precipitated with $AuCl_y(OH)_{3-y}$ (denoted as Au_p) and occluded with the complexes (denoted as Au_o) of $AuCl(OH)_3^-$ and $Au(OH)_4^-$. Conceivably, a large fraction of Au_o would remain in the pores, along with Au_p, during the filtration and washing steps and then deposit there on freshly prepared samples.

A deposition of 2 wt% of gold was intended on preparation of samples. However, the amount of gold actually deposited on prepared samples varied with the surface area of the support. Only 20% of the gold in the $AuCl_3$ solution was deposited on anatase support (S.A. = 47 m^2/g). The deposited fraction increased to 50% on amorphous TiO_2

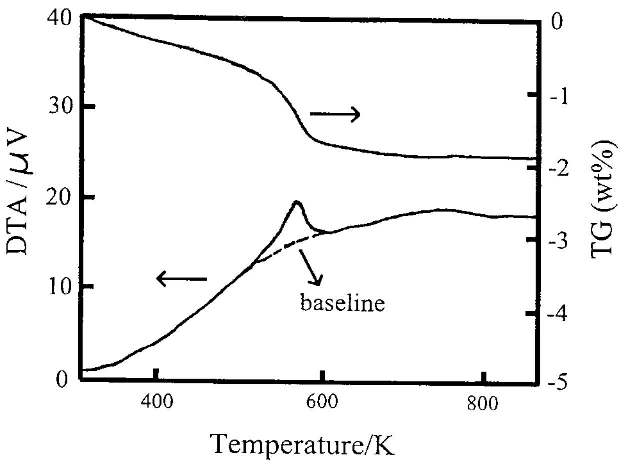

FIG. 6. TG/DTA spectra of fresh NC sample.

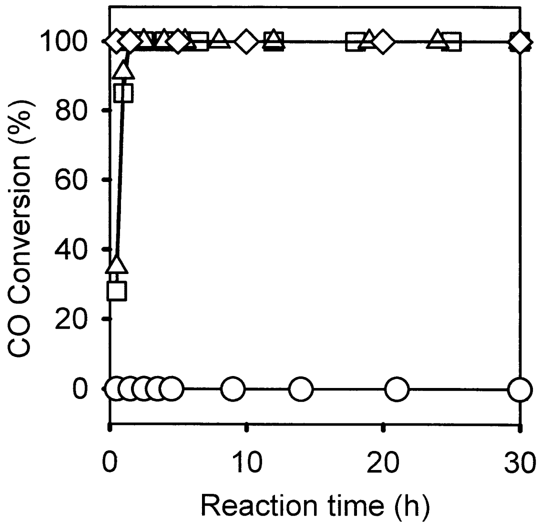

FIG. 7. Time profile of CO conversion in CO oxidation at 273 K over fresh catalysts: ○, AD and AM; △, ND; □, MD; ◇, MC, NC, and AC.

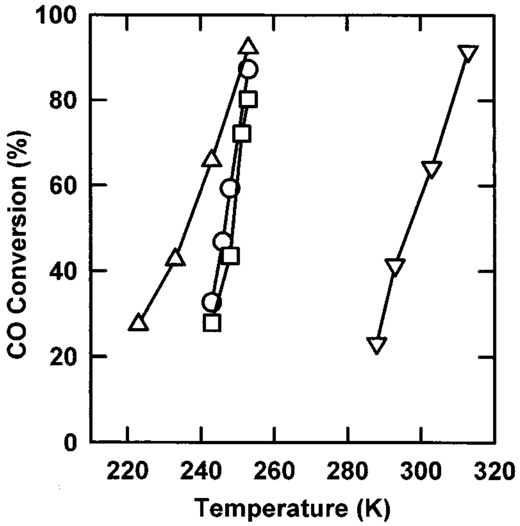

FIG. 9. Temperature profile of catalytic activity of reduced samples prepared by DP method: △, AM; ▽, AD; ○, MD; □, ND.

(S.A. $= 140\ m^2$) and 66% on Al_2O_3 (S.A. $= 234\ m^2/g$). The rest of the gold was either deposited on the surface of the beaker and the stirrer or lost in the filtrate solution.

The fifth column of Table 1 compares the average particle sizes (*d*) of gold on freshly prepared samples. Apparently, DP is an excellent method for preparing highly dispersed Au/TiO_2 samples ($d < 5$ nm for both MD and ND samples). But Au/Al_2O_3 sample (AD) prepared by the traditional DP method showed poor dispersion ($d > 7$ nm). The difference in gold dispersion may be a result of the isoelectric point of these two supports.

4.3. The Effect of Surface Acidity on Au Deposition

The surface of TiO_2 has an isoelectric point of pH 6. The pore surface of this support was therefore negatively charged during suspension in the distilled water (pH 7) and expelled the negatively charged ions. At least two kinds advantages toward a high gold dispersion may be imagined from the anion repulsion. First, fewer Cl^- ions were adsorbed on the surface during the DP process and, consequently, a sintering of gold species would be less probable in the subsequent treatment of drying and calcination. Second, the concentration of Au_o solution occluded in pores of suspended TiO_2 should therefore be lower than that in the filtrate. Consequently, Au_p would be favored over Au_o as the major source of gold deposited on the freshly prepared Au/TiO_2. The aggregates of deposited Au_p would finally

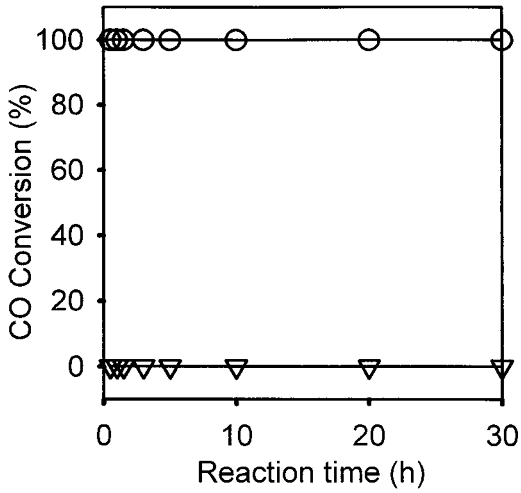

FIG. 8. CO conversion over prereduced samples at 273 K: ○, ND, MD, and AM; ▽, AD.

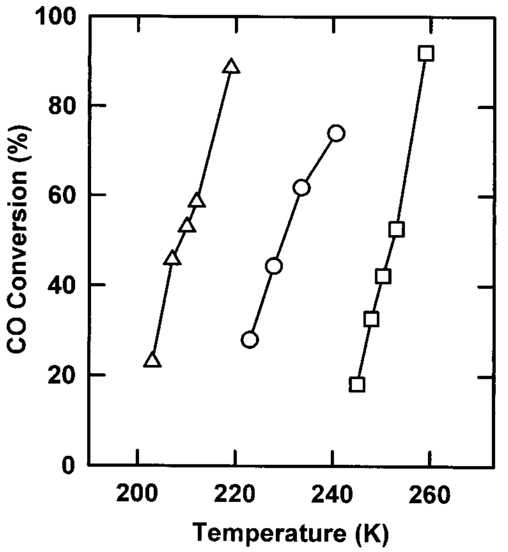

FIG. 10. Temperature profile of catalytic activity of calcined samples prepared by CVD method. △, MC; ○, NC; □, AC.

convert, along with a minor fraction of Au_o, to finely dispersed gold particles in fresh samples.

On the other hand, the surface of Al_2O_3 (with an isoelectric point of pH 8) suspended in deionized water was positively charged and should attract negatively charged ions into the pores during the precipitation deposition and result in a low Au dispersion to AD sample. In the modified DP method, the surface of the Al_2O_3 support was preadjusted to pH 7.0 with diluted NaOH solution before adding $AuCl_3$ solution. The density of the positive charge on the pore surface of Al_2O_3 should have been significantly reduced in the precipitation step. Consequently, the average size of gold particles dispersed on the fresh AM was reduced to 3.4 nm (from 7.2 nm for sample AD).

4.4. The Reduction of Gold Species

Among the gold species on supported Au catalysts prepared by the DP method, $Au(OH)_3$ and $Au(OH)_4^-$ of deposited gold species are thermally unstable at 373 K (16) and tend to decompose into metallic gold during the drying pretreatment:

$$2Au(OH)_3 \rightarrow 2Au + 3H_2O + \frac{3}{2}O_2. \qquad [3]$$

The existence of reduced gold in the dried samples agrees with the gold fringes occasionally found in the transmission electron micrograph (Fig. 3j). Accordingly, the dominant gold species remaining on the dried sample should be the chloride-contaminated gold species (mainly $AuCl_y(OH)_{3-y}$). It is therefore of interest to determine the minimum temperature required for reduction of this chloride-contaminated gold to metallic gold.

Figure 5 compares TPR traces obtained for four fresh samples prepared by the DP method. Only a single reduction peak was noted in each trace. Conceivably, the observed peak may be assigned to reduction of chloride-contaminated gold species such as:

$$2AuCl(OH)_2 + 3H_2 \rightarrow 2Au + 4H_2O + 2HCl. \qquad [4]$$

From the stoichiometric relation of this reaction, the fraction of gold deposited as chloride-contaminated $Au(OH)_3$ in prepared samples could be estimated as $N_{H_2}/1.5N_{Au}$ (where N_{H_2} denotes the number of hydrogen molecules consumed in TPR). The seventh column of Table 1 compares the $N_{H_2}/1.5N_{Au}$ ratios obtained from TPR traces. Around 40% of the gold was deposited with chloride ions for all samples. The rest may be $Au(OH)_3$ species which decompose into metallic gold during the drying treatment.

The minimum temperature (T_r) required for complete reduction of reaction [4] varied significantly in Fig. 4 with the catalyst support. Titania-supported samples (MD and ND) displayed a T_r of 373 K while alumina-supported samples (AD and AM) had a T_r of 473 K. The discrepancy in T_r agrees with the knowledge that alumina is an insulator and titania is an *n*-type support, and *n*-type oxides tend to promote reduction of dispersed cations.

4.5. Activation of Fresh Catalysts

On heating at 343 K, the organic DMGAA complex of gold was vaporized and adsorbed onto the surface of supports through the vacuum system. From TG/DTA spectra of the fresh NC sample (Fig. 5), organic ligands of the adsorbed complex were oxidized in air at 573 K. Accordingly, calcination at $T_c = 573$ K for gold catalysts prepared by the CVD method (MC, AC, and NC) is chosen as the standard procedure for their activation.

Although Au/TiO_2 catalysts (MD and ND) exhibited 100% conversion of CO at 273 K after a 2-h incubation period (Fig. 7), fresh Au/Al_2O_3 (AD and AM) remained inactive even after 30 h of reaction under the same conditions. The observed difference in activation between Au/TiO_2 and Au/Al_2O_3 may be related to their reducibility noted in TPR traces. Samples of Au/TiO_2 and Au/Al_2O_3 are seen in Fig. 5 to be reduced through reaction [4] at 373 and 473 K, respectively, by hydrogen in the TPR flow. CO was found to be more active than H_2 for the oxidation reaction on gold catalysts in literature reports (3, 17), and activation of Au/TiO_2 by a reactant flow of $CO + O_2$ has been reported (15). Conceivably, chloride-contaminated $Au(OH)_3$on Au/TiO_2 may be reduced by CO in the reactant flow at 273 K through

$$2AuCl(OH)_2 + 3CO \rightarrow 2Au + 2HCl + H_2O + 3CO_2. \qquad [5]$$

It is therefore our proposal that chloride ions in deposited gold salts inhibit reaction [1] and that the activation of these catalysts involves mainly the reduction of gold salt into the metallic state.

Since more severe conditions are required for the hydrogen reduction of Au/Al_2O_3 than for Au/TiO_2, the reduction by the reactant flow at 273 K may be too mild for substantial activation of Au/Al_2O_3. In Fig. 8, an AM sample prereduced at 473 K indeed exhibited good activity without any induction period. We may therefore be confident that decent reduction of reaction [4] can activate gold catalyst prepared from $AuCl_3$ precursor and TPR is a good technique to determine the conditions (T_r) required by the reduction.

4.6. The Effect of Gold Particle Size with Catalytic Activity

According to the TPR results in Fig. 5, Au/Al_2O_3 samples can be completely reduced in the hydrogen flow at 473 K. Surprisingly, the reduced AD remained inactive toward CO oxidation at a reaction temperature of 273 K (Fig. 8). On examination of the physical properties of the prepared samples (Table 1), the diameter of gold on catalyst AD (7.2 nm) is somewhat larger than those (<5.0 nm) of the

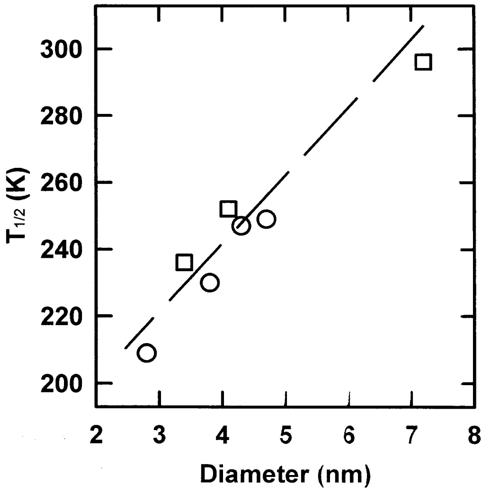

FIG. 11. Relation between gold cluster diameter and $T_{1/2}$: □, Au/Al_2O_3; ○, Au/TiO_2.

other catalysts prepared. Evidently, the gold particles on sample AD were too large to catalyze the CO oxidation at 273 K. The temperature profile in Fig. 9 further demonstrates that reasonable activity of the AD sample required a reaction temperature of 280 K or higher.

Figure 11 correlates $T_{1/2}$ (the temperature at which 50% CO conversion occurs under our reaction conditions) measured in the activity test with the particle size of samples characterized in this study. The observed $T_{1/2}$ generally increases with the average size of gold particles dispersed. A dependence of catalytic activity on particle size is indeed confirmed. Evidently, the oxidation of CO over gold catalyst is a structure-sensitive reaction.

The observed effect of particle size of gold on its activity has been established in the literature for quite a long time (3, 4). Although different explanations have been proposed for this effect, the following Langmuir–Hinshelwood mechanism is generally accepted:

$$CO + * \rightarrow *\text{–}CO \quad [6]$$

$$O_2 + * \rightarrow *\text{–}O_2 \quad [7]$$

$$CO\text{–}* + O_2\text{–}* \rightarrow CO_2 + O\text{–}* + * \quad [8]$$

$$O\text{–}* + CO\text{–}* \rightarrow CO_2 + 2*. \quad [9]$$

Since both reactants, i.e., O_2 and CO, are weakly adsorbed on Au, the rate of reaction should be proportional to the coverage of these reactants, θ_{CO} and θ_{O_2}, on gold catalysts.

Haruta *et al.* found evidence (4, 7, 18) that active sites of reactant adsorption are located at the interface between the support and the dispersed gold. They attributed size effect to an increase in the interface perimeter (or a density of adsorbed reactant on catalysts). Baiker *et al.* reported that the rate of CO conversion is higher for gold catalysts supported by *n*-type semiconductors than for those dispersed on insulator (19). They suggested that O_2 molecules were adsorbed mainly at the defect sites of the *n*-type semiconductor and that a diffusion of adsorbed O_2 to CO adsorbed at nearby gold particles is the rate-determining step of CO oxidation (20). Goodman *et al.*, in a recent scanning tunneling microscope study, found a gradual shift in electric conductivity of gold particles dispersed on a single crystal of TiO_2. They regarded the size effect as a consequence of the shift of the electronic conductivity of nanogold from conductor to semiconductor (21).

4.7. The Effect of Support with Catalytic Activity

We cannot assess the relative contributions of these explanations from the results of the present study. Nevertheless, Fig. 11 does illustrate that the activity of the Au/Al_2O_3 sample is indeed lower than that of the Au/TiO_2 sample with a similar size of gold. Column 4 in Table 1 further demonstrated that the loading of Au does not significantly affect $T_{1/2}$ of reaction [1]. Obviously, it is the size of gold particles, rather than the nature of support or the density of reactants adsorbed on catalysts, that plays a major role in the variation of activity.

Vannice *et al.* found that the heat of adsorption (for hydrogen and oxygen) on dispersed Pt and Pd increases significantly on decreasing the particle size to less than 5 nm (22, 23). Variation in the chemical and physical (color, audio, etc.) properties has also been proposed for materials in this nanoparticle range (24). The observed high activity of gold particles with diameters less than 5 nm, in our opinion, may be attributed to an increase in the affinity of these particles to the weakly adsorbed reactants (CO and O_2) or an increase in θ_{CO} and θ_{O_2} on gold catalysts.

It is also noteworthy that Haruta *et al.* (17) have successfully prepared a highly dispersed Au/Al_2O_3 catalyst with the traditional DP method. The reported $T_{1/2}$ (290 K) for the catalytic CO oxidation for their catalyst is similar to that (296 K) found in this study for catalyst AD. These two catalysts were prepared by a common procedure of precipitating gold complexes to the Al_2O_3 surface at pH 7. In this study, pretreatment of the Al_2O_3 surface with NaOH before the precipitation step led to a very active Au/Al_2O_3 catalyst (AM, $T_{1/2} = 236$ K). The enhanced activity may result from, besides the high Au dispersion mentioned in Section 4.3, the prevention of Cl^- deposition on the Al_2O_3 surface.

Sanchez *et al.* (25) studied the effects of defects in MgO support on the catalytic properties of Au/MgO catalyst. They suggest that defects may promote the activity of the catalyst toward CO oxidation. In the present study, we found a slightly lower $T_{1/2}$ for Au/TiO_2 in reaction [1] than for Al_2O_3. The high activity observed for Au/TiO_2 may be attributed partially to the *n*-type nature of the TiO_2 support.

CONCLUSIONS

1. Small gold particles ($d_{Au} < 5$ nm) have been successfully deposited on Al_2O_3 support by the modified DP method. The prepared catalyst displays good catalytic activity toward CO oxidation at subambient temperatures.

2. Reduction of gold complex to metallic gold is required for activating gold catalysts prepared by the DP method. The support of gold catalysts profoundly affects the reducibility of dispersed chloride-contaminated gold hydroxides ($AuCl_y(OH)_{3-y}$). The 2-h incubation time found in Fig. 7 for CO oxidation at 273 K over fresh Au/TiO_2 is required for reduction of the contaminated hydroxides into metallic gold. Similar activation of Au/Al_2O_3 cannot be achieved under the same reaction conditions but may be accomplished by a reduction with hydrogen at 473 K.

ACKNOWLEDGMENTS

The authors acknowledge financial support for this study from the Nation Science Council of the Republic of China through Contract NSC-88-2113-M-007-027. Helpful discussions with Professor S. D. Lin of Yuan-Ze University are also appreciated.

REFERENCES

1. Wachs, I. E., *Gold Bull.* **16**, 98 (1983).
2. Schwank, J., *Gold Bull.* **18**, 2 (1985).
3. Haruta, M., Yamada, N., Kobayashi, T., and Iijima, S., *J. Catal.* **115**, 301 (1989).
4. Haruta, M., Tsubota, S., Kobayashi, T., Kageyama, H., Genet, M., and Delmon, B., *J. Catal.* **144**, 175 (1993).
5. Haruta, M., Kobayashi, T., Sano, H., and Yamada, N., *Chem. Lett.*, 405 (1987).
6. Tsubota, S., Haruta, M., Kobayashi, T., Ueda, A., and Nakahara, Y., *in* "Preparation of Catalysts V" (G. Poncelet *et al.*, Eds), p. 695. Elsevier Science, Amsterdam, 1991.
7. Tsubota, S., Cunningham, D. A. H., Bando, Y., and Haruta, M., *in* "Preparation of Catalysts VI" (G. Poncelet, *et al.*, Eds), p. 227. Elsevier Science, Amsterdam/New York, 1995.
8. Bamwenda, G. R., Tsubota, S., Nakamura, T., and Haruta, M., *Catal. Lett.* **44**, 83 (1997).
9. Yuan, Y., Asakura, K., Wan, H., Tsai, K., and Iwasawa, Y., *Catal. Lett.* **42**, 15 (1996).
10. Okumura, M., Tanaka, K., Ueda, A., and Haruta, M., *Solid State Ionics* **95**, 143 (1997).
11. Iizuka, Y., Fujiki, H., Yamauchi, N., Chijiiwa, T., Arai, S., Tsubota, S., and Haruta, M., *Catal. Today* **36**, 115 (1997).
12. Grunwaldt, J. D., Kiener, C., Wogerbauer, C., and Baiker, A., J. *Catal.* **181**, 223 (1999).
13. Chang, C. K., Chen, Y. J., and Yeh, C. T., *Appl. Catal. A* **174**, 13 (1998).
14. Lin, S. D., Bollinger, M., and Vannice, M. A., *Catal. Lett.* **17**, 245 (1993).
15. Dekkers, M. A. P., Lippits, M. J., and Nieuwenhuys, B. E., *Catal. Lett.* **56**, 195 (1998).
16. Budavari, S., *et al.* (Eds.), *in* "The Merck Index," 12th ed., p. 4539. Merck & Co., Whitehouse Station, NJ, 1996.
17. Okumura, M., Nakamura, S., Tsubota, S., Nakamura, T., Azuma, M., and Haruta, M., *Catal. Lett.* **51**, 53 (1998).
18. Boccuzzi, F., Chiorino, A., Tsubota, S., and Haruta, M., *J. Phys. Chem.* **100**, 3625 (1996).
19. Grunwaldt, J. D., Maciejewski, M., Becker, O. S., Fabrizioli, P., and Baiker, A., *J. Catal.* **186**, 458 (1999).
20. Grunwaldt, J. D., and Baiker, A., *J. Phys. Chem.* **B 103**, 1002 (1999).
21. Valden, M., Lai, X., and Goodman, D. W., *Science* **281**, 1647 (1998).
22. Sen, B., and Vannice, M. A., *J. Catal.* **129**, 31 (1991).
23. Wang, C. B., and Yeh, C. T., *J. Catal.* **178**, 450 (1998).
24. Sigel, R. W., Hu, E., and Roco, M. C., *in* "Nanostructure Science and Technology," TWEC. Loyola College, MD, 1999.
25. Sanchez, A., Abbet, S., Heiz, U., Schneider, W. D., Häkkinen, H., Barnett, R., Barnett, N., and Landman,U., *J. Phys. Chem. A* **103**, 9573 (1999).